Journal of Engineering Sciences and Information Technology (JESIT) • Vol 9, Issue 4 (2025) • P: 34 - 19
https://journals.ajsrp.com/index.php/jesit
ISSN: 2522-3321(Online) • ISSN: 2522-3321(Print)

Improving the Mechanical Properties of Hypereutectic Al–14%Si Alloy by Adding Alumina Particles of Different Sizes Using the Taguchi Method

Eng. Farah. Ammar Ibrahim*, Prof. Zeyad D. Kadhim, Prof. Mohammed Abdulraoof Abdulrazzaq
College of Engineering | Mustansiriyah University | Iraq

Received: 02/09/2025
Revised: 15/09/2025
Accepted: 05/10/2025
Published: 15/12/2025

* Corresponding author: farahammar@uomustansiriyah.edu.iq

Citation: Ibrahim, F. A., Kadhim, Z. D., & Abdulrazzaq, M. A. (2025). Improving the Mechanical Properties of Hypereutectic Al–14%Si Alloy by Adding Alumina Particles of Different Sizes Using the Taguchi Method. *Journal of engineering sciences and information technology, 9*(4), 19 – 34. https://doi.org/10.26389/AJSRP.B040925

2025 © AISRP • Arab Institute for Sciences & Research Publishing (AISRP), United States, all rights reserved.

• **Open Access**

This article is an open access article distributed under the terms and conditions of the Creative Commons Attribution (CC BY-NC) license

Abstract: This study examines how adding 3 weight percent Al_2O_3 particles with different particle sizes (25 µm, 50 µm, and 100 µm) using the stir casting technique can improve the mechanical and tribological characteristics of a hypereutectic Al–14%Si alloy. To create the composites, preheated Al_2O_3 particles were evenly distributed throughout the molten Al–Si alloy and solidified carefully. Vickers hardness and pin-on-disc dry sliding wear tests were used to assess the mechanical performance, whereas optical microscopy (OM), scanning electron microscopy (SEM), and X-ray diffraction (XRD) were used to characterise the microstructures. The Taguchi L9 orthogonal array design was used to systematically optimise the experimental parameters, such as the particle size, applied load, and sliding time. The effects of these parameters on the wear behaviour were examined using ANOVA. The finest 25 µm particles achieved the most uniform distribution and the highest hardness of 110 HV, compared to 92 HV for the unreinforced alloy. The results showed that the addition of Al_2O_3 significantly improved the particle–matrix interface and refined the grain structure of the composites. A strong correlation between increased surface hardness and decreased wear rate was confirmed by the wear resistance, which significantly improved as the particle size decreased. According to the statistical analysis, the most important factors influencing the wear rate were particle size, applied load, and sliding time. This study demonstrates how optimising the particle size can improve the performance of Al–Si– Al_2O_3 composites. High wear resistance and durability are crucial for demanding applications in automotive, aerospace, and industrial components, and these composites show great promise owing to their fine particle reinforcement and optimised processing conditions.

Keywords: Stir Casting; Taguchi's Techniques; Wear; Hypereutectic Al-14%SI.

تحسين الخواص الميكانيكية لسبيكة الألمنيوم–14% سيليكون فوق اليوتكتيكية بإضافة جسيمات ألومينا ذات أحجام مختلفة باستخدام طريقة تاكوجي

المهندسة / فرح عمار إبراهيم*، الأستاذ الدكتور/ زياد دوشان كاظم، الأستاذ الدكتور/ محمد عبد الرؤف عبد الرزاق
كلية الهندسة | الجامعة المستنصرية | العراق

المستخلص: تبحث هذه الدراسة في كيفية تأثير إضافة جسيمات Al_2O_3 بنسبة 3% وزناً وبأحجام مختلفة (25 ميكرومتر، 50 ميكرومتر، و100 ميكرومتر) باستخدام تقنية الصب بالتحريك على تحسين الخصائص الميكانيكية والتريبولوجية لسبيكة الألمنيوم فائقة اليكتكتية (Al–14%Si). جرى تحضير المواد المركبة من خلال توزيع جسيمات Al_2O_3 المسخّنة مسبقًا بشكل متجانس داخل مصهور سبيكة الألمنيوم–السيليكون ثم تبريدها بعناية. تم تقييم الأداء الميكانيكي باستخدام اختبار الصلادة فيكرز واختبار التآكل الجاف بطريقة القرص–الدبوس، بينما جرى توصيف البنية المجهرية باستخدام المجهر الضوئي (OM) والمجهر الإلكتروني الماسح (SEM) وحيود الأشعة السينية (XRD). كما استُخدم تصميم مصفوفة أورثوغونال Taguchi L9 للتحسين المنهجي لمتغيرات التجربة، مثل حجم الجسيمات، الحمل المسلط، وزمن الانزلاق. وتم تحليل تأثير هذه العوامل على سلوك التآكل باستخدام تحليل التباين (ANOVA). أظهرت النتائج أن الجسيمات الدقيقة بحجم 25 ميكرومتر حققت أفضل توزيع وأعلى صلادة بلغت 110 HV مقارنة بـ 92 HV للسبيكة غير المدعمة. وأكدت النتائج أن إضافة Al_2O_3 ساهمت بشكل ملحوظ في تحسين الواجهة بين الجسيمات والمصفوفة وتنقية البنية الحبيبية للمواد المركبة. كما أثبتت مقاومة التآكل وجود ارتباط قوي بين زيادة الصلادة السطحية وانخفاض معدل التآكل، حيث تحسنت مقاومة التآكل بشكل كبير مع تقليل حجم الجسيمات. وبحسب التحليل الإحصائي، كانت أهم العوامل المؤثرة في معدل التآكل هي حجم الجسيمات، الحمل المسلط، وزمن الانزلاق. وتبرهن هذه الدراسة أن تحسين حجم الجسيمات يمكن أن يعزز أداء المواد المركبة من Al–Si–Al_2O_3 ، حيث تعد المقاومة العالية للتآكل والمتانة ضرورية للتطبيقات ذات المتطلبات العالية في مجالات السيارات والطيران والمكونات الصناعية. وتُظهر هذه المواد المركبة آفاقاً واعدة بفضل تعزيزها بالجسيمات الدقيقة وظروف المعالجة المثلى.

الكلمات المفتاحية: الصب بالتحريك؛ تقنيات تاغوتشي؛ التآكل؛ سبيكة Al–14%Si فائقة اليوتيكتك.

1. Introduction

The binary aluminum-silicon system serves as the foundation for (aluminum-silicon)casting alloys, in which silicon is the predominant alloying component. These alloys, referred to as (silumins,) account for more thanNinety percent of all castings made from aluminum. Al-SiAlloys are employed as construction materials across a range of applications and function as a soldering agent for aluminum,exemplified by (Al-Ge.) Heat-resistant aluminum alloys are used in automotive engine components, including connecting rods, rocker arms, cylinders, pistons, and valve retainers [L. Lasaj et al. .2003, Zhao Qian et al. .2008]. Furthermore, aluminum metal matrix composites (AMMCs) are significant owing to their cost-effectiveness, widespread availability, and casting capability [Afnan Haider Khan et al.2022 - Dipti Kanta Das et al.2014- Ideris Muhammad Haziq et al.2023]. Aluminum-silicon alloys are significant because of their excellent strength-to-weight ratio, superior wear resistance, low thermal expansion coefficient, high thermal conductivity, remarkable corrosion resistance, favourable casting properties, and good weldability [P. V. Chandra Sekhar Rao et al.2012, Rahul Gope et al.2024]. The mechanical characteristics of Al–Si alloys are significantly influenced by the distribution and morphology of silicon particles. Silicon is regarded as beneficial in metallic alloys because it enhances melt fluidity, lowers melting temperatures, reduces shrinkage during solidification, and is relatively expensive as a raw material [S. K. Dey et al.2109, Muhammad Hisyamuddin Rosli et al.2025]. Al-Si alloys can be classified based on their silicon content into hypoeutectic (less than 12% Si), hypereutectic (more than 12% Si), or eutectic (exactly 12% Si) [Nan Kang et al.2016, Q. Z. Wang et al.2020]. Alumina

(Al_2O_3), boron carbide (B4C), and silicon carbide (SiC) are the predominant ceramic materials investigated for the improvement of Al-Si composite properties [Bharat KumarJyot–et al.2016 - N. Radhika et al.2024- Muhammad Faiz Abdul Razak et al.2024]. Casting is a cost-effective method compared to other production techniques, and stir casting is often acknowledged as a commercially validated approach. Furthermore, stir casting facilitates the substitution and incorporation of conventional metal processing methods, leading to cost reductions in the overall process. However, when employing the stir casting technique for the production of metal matrix composites, it is essential to meticulously consider several factors, such as the challenge of achieving an adequate allocation of reinforcement materials and the porosity found within the cast metal matrix composites [Ashish Kumar et al.2020]. Using the stir-casting technique, the researchers systematically incorporated the components to attain the target composition for the composites. They examined the physical properties associated with the mechanical performance of metal matrix composites, focusing on parameters such as hardness and tensile strength [Pitchayyapillai et al.2017]. Casting Al-Si alloys results in diverse morphologies, and incorporating reinforcements, such as alumina, refines the grain structure and enhances the microstructural, wear, and mechanical properties. Traditional casting methods for hypereutectic Al-Si alloys result in diverse microstructural morphologies. The distribution of shape and size is crucial for determining mechanical and tribological characteristics. The increased alumina content within the aluminum matrix contributed to improved strength, hardness, and consistent displacement [Sahu et al.2022–Nordin et al.2024]. Although many studies have examined the improvement of hypereutectic Al–Si alloys by adding ceramic reinforcements such as SiC, B_4C, and Al_2O_3, most of the available research has concentrated on either nanoparticles or alloys with silicon contents below 12% (hypoeutectic) or precisely at the eutectic composition. Hypereutectic Al–Si alloys with 14% silicon have received little attention despite their potential for superior wear resistance and thermal stability in demanding applications, such as automotive and aerospace components. Furthermore, prior research frequently lacked a methodical optimization approach to investigate the combined effects of important process parameters on the mechanical and tribological behaviours of these composites, including particle size, applied load, and sliding time. For instance, many studies have used partial factorial designs or conventional trial-and-error techniques, which are not very good at capturing how variables interact. The microstructural characterization and its direct relationship with mechanical performance represent another research gap. For hypereutectic Al–14%Si systems, a thorough statistical analysis combined with Taguchi's orthogonal array design and sophisticated ANOVA techniques to identify the most influential parameters has rarely been explored, despite prior studies reporting improvements in hardness and wear resistance with the addition of Al_2O_3. Furthermore, thorough analyses relating the observed increases in hardness and wear resistance to microstructural refinement, phase stability (as demonstrated by XRD), and interfacial bonding (as observed by SEM) are lacking. Therefore, studies that not only report experimental findings but also offer comprehensive explanations of how the particle size and distribution affect the overall performance of the alloy are urgently required. By employing a statistically optimized Taguchi design in conjunction with comprehensive microstructural, mechanical, and tribological analyses, this study fills these gaps by methodically examining the effects of various Al_2O_3 particle sizes (25, 50, and 100 μm) to establish a strong correlation between the processing parameters, microstructure, and the performance

[Tirfe et al. 2024] investigated the effect of key tribological parameters—namely applied load, rotational speed, and reinforcement weight percentage—on the dry sliding wear rate of a stir-cast Al6061 hybrid composite reinforced with nano-Al_2O_3 and quartz particles. Using a Taguchi L27 orthogonal array and ANOVA, they found that the applied load had the most significant impact (87.83%) on the wear rate, followed by the rotational speed (10.06%) and reinforcement percentage (1.60%). The developed regression model showed a positive correlation between the wear rate and both the load and speed, and a negative correlation with the reinforcement percentage. They also observed that increasing the quartz content increased the porosity of the composite.. In a recent study,[Subramanian et al. 2025] investigated the dry sliding wear behaviour of aluminum metal matrix composites (AMMCs) based on an Al6061 alloy reinforced with silicon carbide (SiC) particles. The composites were fabricated using the stir casting method, with SiC particles of average size 44 µm added at varying weight percentages (0%, 3.5%, and 7.0%). Wear experiments were conducted under different loads (10–30 N), sliding distances (1000–3000 m), and sliding velocities (1.5–3.5 m/s). The experimental design was carried out using the Taguchi orthogonal array method, and the results were analysed using Analysis of Variance (ANOVA) to evaluate the influence of the process parameters. The findings revealed that the addition of SiC particles significantly enhanced the wear resistance of the composite, making it suitable for applications that require a high strength-to-weight ratio.

This study investigates the reinforcement of aluminum silicon alloys with Al_2O_3 through a method of stir casting, examining the effects of this additive affecting the wear resistance, hardness, and microstructural characteristics of the aluminum silicon alloy

In light of the aforementioned points, there is a distinct necessity for a methodical investigation focused on enhancing the characteristics of Al–14%Si alloys through the integration of Al_2O_3 particles of varying dimensions, while examining the correlation between particle distribution and the mechanical, tribological, and microstructural attributes of the alloy. Consequently, the primary research question is as follows:

"What impact do the size of Al_2O_3 particles, the applied load, and the duration of sliding have on the mechanical and wear properties of Al–14%Si alloy when processed via the stir casting method?"

To address this enquiry, this study aims to:

1. Metal matrix composites of Al–14%Si alloy reinforced with Al_2O_3 particles measuring 25, 50, and 100 µm were fabricated.
2. The influence of particle size on the hardness and wear rate under dry sliding conditions was assessed.
3. The Taguchi design and ANOVA were used to statistically determine the most significant factors influencing the wear behaviour.
4. The relationship between the microstructure (through OM, SEM, and XRD) and mechanical properties was investigated to elucidate the mechanisms responsible for performance enhancement.

This study aims to bridge the existing gap in the literature by offering a thorough experimental and analytical framework that deepens the understanding of the interaction between the processing parameters and the properties of ceramic-reinforced aluminum–silicon alloys.

2. Experimental Work

2.1 Materials

High-purity silicon (Si) and aluminum (Al) metals were used as base materials to create composite specimens, and alumina (Al_2O_3) ceramic reinforcement was added. A hypereutectic Al–14%Si composition of the base alloy was created to guarantee a balance between the high wear resistance and desired mechanical strength. Table 1 shows the chemical composition of the hypereutectic Al–Si alloy, with aluminum making up the remaining 14% and minor alloying elements such as Fe, Cu, Mg, Ti, and trace impurities, respectively.

To ensure minimal contamination during processing, commercial-grade silicon with a purity of 99.5% and aluminum with a purity of 99.7% were used. The reinforcement material was composed of high-purity (>99.8%) Al2O3 powders with controlled particle sizes of 25, 50, and 100 µm to guarantee consistency in the experiments. To assess the impact of the reinforcement scale on the microstructural, mechanical, and wear properties of the composites, particle sizes were selected for the study. Coarser 100 µm particles were added to evaluate the effects of decreased surface area and possible agglomeration during processing, whereas the finer 25 µm Al_2O_3 particles were anticipated to improve the interfacial bonding and grain refinement of the composites.

To remove moisture and avoid gas porosity during casting, the reinforcement particles were meticulously preheated to 250°C before being added to the melt. Stir casting, a popular and affordable method for creating metal matrix composites (MMCs) owing to its ease of use, scalability, and potential to achieve a uniform particle distribution with optimization, was used for the fabrication process. The hypereutectic Al–Si alloy was created by first melting the aluminum at a regulated temperature in a clay-bonded graphite crucible and then gradually adding silicon. To guarantee uniform dispersion of the particles within the matrix, the molten alloy was continuously

stirred with a mechanical stirrer at 450–500 rpm for 10 min after the base melt was homogenised. Preheated Al_2O_3 powders were added as a reinforcement at a concentration of 3% wt .

All instruments that came into contact with the molten alloy were preheated to avoid sharp temperature drops during mixing, and the entire procedure was performed under a protective cover flux to reduce oxidation. Subsequently, the molten slurry was poured into cast iron moulds that had been heated to approximately 300°C to prevent porosity and early solidification. The consistent composition and microstructure of the finished composites were guaranteed by this controlled processing method, which qualified them for further testing of wear resistance, hardness, and microstructural characteristics.

2.2 Hypereutectic Al-Si Composite Specimen Preparation

The procedure involved placing aluminum wires into a clay-bonded graphite crucible, which was subsequently heated in a gas furnace until the aluminum melted. Once melted, pure commercial silicon was introduced and thoroughly mixed using a graphite mixer until it fully dissolved in the molten aluminum. Additionally, 3% alumina (Al_2O_3) with particle sizes of 25, 50, and 75 μm was incorporated [Bhutto et al.2025]. Subsequently, an aqueous solution of aluminum chloride was added to the molten aluminum at a concentration of 1 g/L. The mixture was briefly stirred, after which the slag was removed. The resulting mixture was poured into a preheated cast iron mould at 300°C to prevent rapid solidification and avoid pore formation. A cast rod with a diameter of 14 mm and a length of 22 cm was produced. To achieve a homogeneous structure, the cast rod was placed in an electrical furnace at 500°C and allowed to cool in air within the furnace, facilitating the development of a uniform grain structure.

Table 1: Chemical composition of Al-Si alloy.

Element	Si%	Fe%	Cu%	Mn%	Mg%	Cr%	Ni%	Zn%	Ti%	Pb%	Al%
Al-Si alloy	14	0.51	0.01	0.007	0.019	0.01	0.021	0.019	0.018	0.0005	Bal

2.3 Microstructure Test

The metal samples were cut to a length of 20 mm and ground with emery papers rated 220, 400, 600, 800, 1000, 1200, 1500, and 2000. Water was used to prevent the heat from worsening the condition. Diamond paste was used to smooth the samples, which were then placed in Keller's solution for 15 s. The solution was composed of 1 ml HF, 1.5 ml HCl, 2.5 ml HNO3, and 95% water. Subsequently, alcohol and water were used to clean the samples, which were then dried using hot air was used to dry them. The samples were then ready for examination [Varun Singhal et al.2024].

2.4 The Scanning Electron Microscope

To examine the findings related to the microstructure of Al-Si alloys following the addition of Al2O3, a Scanning Electron Microscopy (SEM) analysis was conducted.

2.5 Hardness Test

Vickers hardness testing was employed in this study to assess the hardness of the samples. A load of (1) kg was applied for 15 s, after which the penetration diameter was determined using the following equation [Ahmed J. Abuzinadahet al.2024]

$$Hv = 1.854 \times P / d\,(Av)^2 \qquad (1)$$

Where:

Hv: Represents the Vickers hardness

(P): The symbol denotes the load in kilograms and

d(Av): Indicates the depth of penetration.

2.6 Wear Test

In the current study, a pin-on-disc apparatus was used for wear measurements. The samples were prepared with a length of 30 mm and diameter of 10 mm. Three different loads (10, 15, and 20 N) were applied, Al_2O_3ng with a sliding velocity of 340 m/s, over varying durations of (10, 15, and 20 min).

The wear rate for the samples was determined using the following equation [Md Jalal Uddin Rumiet al.2023]:

$$Wear\ rate\ (w.r) = \Delta w / \pi DNt \quad (2)$$

Where:

Δ w = (w0-w1)

D: Sliding distance (14 cm)

T= Time (minutes)

N= Rotational speed (rpm)

2.7 Plan of Experiment

The experiments were conducted using a standard orthogonal array methodology. The selection of the orthogonal array was determined by ensuring that the degrees of freedom associated with the array were greater than or at least equal to the total degrees of freedom for the wear parameters. In this study, an An(L9) orthogonal array was selected., as shown in Table 2. The parameters of wear selected for the experiment included (A) applied load, (B) time, and (C) particle size. The experimental design comprised nine tests, corresponding to each row in the L9 orthogonal array, with columns designated for the parameter values. The first, second, and third columns represent the particle size, applied load, and time, respectively. The experiments were performed according to the orthogonal array, with the parameter levels specified in each row of the array. The experimental results were further analyzed using the signal-to-noise ratio (SNR). The primary response variable examined was the wear rate, with the aim of minimizing this value. The wear rate was computed using a logarithmic transformation of the loss function, as detailed below [D. Elil Rajaet al.2024].

$$(S/N) = -10 \times log\ 1/n\ (\Sigma\ Yi2\ ) \quad (3)$$

The variable 'n' denotes the count of observations, while 'Yi' signifies the recorded values for the wear rate and the coefficient of friction are discussed. It is recommended that the quality characteristics be improved when the signal-to-noise (S/N) ratio is minimized.

Table 2: L9 orthogonal array.

Exp. No	Particle size (µm)	Load (N)	Time (MIN)
1	25	10	10
2	25	15	15
3	25	20	20
4	50	10	15
5	50	15	20
6	50	20	10
7	100	10	20
8	100	15	10
9	100	20	15

Table 3 summarizes the primary experimental parameters used in the Taguchi design to enhance readability and clarity. To assess the impact of each factor on the wear rate, hardness, and microstructural refinement, the factors were systematically changed across three levels.

Table 3: Summary of Experimental Parameters

Factor	Levels Considered	Reference in Analysis
Particle Size (µm)	25, 50, 100	L9 Taguchi Array (Column A)
Applied Load (N)	10, 15, 20	L9 Taguchi Array (Column B)
Sliding Time (min)	10, 15, 20	L9 Taguchi Array (Column C)
Reinforcement Ratio	3 wt.% Al_2O_3	Constant for all samples

3. Results and Discussions

3.1 The influence of Al_2O_3 on the microstructure of AL-Si alloy

Fig 1. microstructure of aluminum – 14% silicon with addition of Al2O3as shown: a) after addition Al_2O_3 with grain size of 25µm; b) after addition Al_2O_3 with grain size of µm100; c) after addition Al_2O_3 with grain size of 50µm

The microstructure of the hypereutectic Al–14%Si alloy was significantly improved and refined by the addition of Al_2O_3 particles. During solidification, fine particles, especially those at 25 µm, were distributed more evenly throughout the aluminum matrix and served as efficient nucleation sites. A more uniform structure was obtained owing to the reduction in grain size, enhancement of particle-matrix bonding, and reduction in porosity. Although the 100 µm particles tended to cluster, resulting in a non-uniform distribution and weaker interfaces, the 50 µm particles offered moderate refinement but exhibited slight agglomeration. These finer particle microstructural improvements account for the increased hardness and wear resistance, which is consistent with earlier research that highlights the importance of particle size in maximizing the performance of Al–Si composites.

3.2 XRD analysis

The X-ray diffraction (XRD) analysis revealed that the primary peaks identified as AL and SI correspond to the presence of Al_2O_3 within the alloy, as illustrated in the results as show in Figure 2and table (4,5,6).

The particle size and dispersion quality within the aluminum matrix were directly related to the phase composition and crystallographic behavior of the hypereutectic Al–14%Si alloy reinforced with alumina (Al_2O_3). wasis as demonstrated by the X-ray diffraction (XRD) analysis of the alloy at 25, 50, and 100 µm thickness. Aluminum (Al) and silicon (Si) were consistently represented by sharp peaks in the diffraction patterns, suggesting that the primary hypereutectic matrix structure was stable in all samples. These peaks are in line with earlier research by Nan Kang et al. (2016) and S. K. Dey et al. (2009), which emphasized the phase stability of Al–Si alloys during processing. They were obtained near 2θ values of approximately 38°, 44°, and 78° for Al, and approximately 28° and 47° for Si. Furthermore, the successful integration of the reinforcement particles into the matrix was confirmed by the appearance of distinct Al_2O_3 peaks near $2\theta \approx 69°$ and 82°, as reported by Bhutto et al. (2025).

The particle size significantly affected the intensity of the Al2O3 3 peaks in the XRD patterns. Sharper and more intense peaks were observed for the alloy reinforced with 25 µm Al_2O_3 particles. This indicates improved dispersion and stronger interfacial bonding within the composite matrix. Enhanced wetting of finer particles during the stir casting process produces a refined microstructure and homogeneous distribution, which in turn leads to improved uniformity. The XRD results for the alloy reinforced with 50 µm particles revealed moderate peak intensities, which were consistent with the microstructural observations and suggested a partially uniform dispersion with some localized agglomeration. In contrast, the alloy with 100 µm particles exhibited weaker and broader Al_2O_3 peaks, suggesting that the larger particles were poorly distributed and clustered, which lowered the interfacial bonding and increased the possibility of microstructural flaws. The results of Bharat Kumar and Menghani (2016), who highlighted that larger particle sizes frequently experience poor wettability and limited bonding during the casting process, were consistent with this observation.

Sharper and better-defined diffraction peaks, which show increased crystallinity and decreased lattice defects, further demonstrate the refinement of the grain structure caused by the addition of finer Al_2O_3 particles. This observation is consistent with the findings of Singhal et al. (2024), who found that finer reinforcements help Al–Si matrix composites achieve better grain refinement and uniformity than coarser reinforcements. The superior mechanical performance of the 25 µm particle size sample, particularly its highest hardness value (110 HV) and improved wear resistance, is strongly correlated with its improved crystallinity and stable phase structure. The significance of uniform dispersion for mechanical enhancement is highlighted by the weaker peaks in the 100 µm particle size sample, which correlates with its lower hardness (95 HV) and decreased wear performance. Nordin et al. (2024) reported similar results, showing that finer reinforcement particles improved mechanical stability and load transfer efficiency.

Overall, the XRD analysis demonstrated that the phase stability and crystalline refinement of the hypereutectic Al–14% Si alloy were significantly influenced by the particle size. The improved mechanical behaviour observed in the hardness and wear tests can be explained by the fine 25 µm particles, which guarantee a more stable and refined structure, improved bonding, and better crystallographic stability of the composites. These

results strongly support the conclusion that improving particle size is essential for attaining superior microstructural and mechanical properties in Al–Si–Al_2O_3 metal matrix composites, and they are consistent with previous research by Bhutto et al. (2025), Sahu et al. (2022), and Rao et al. (2012).

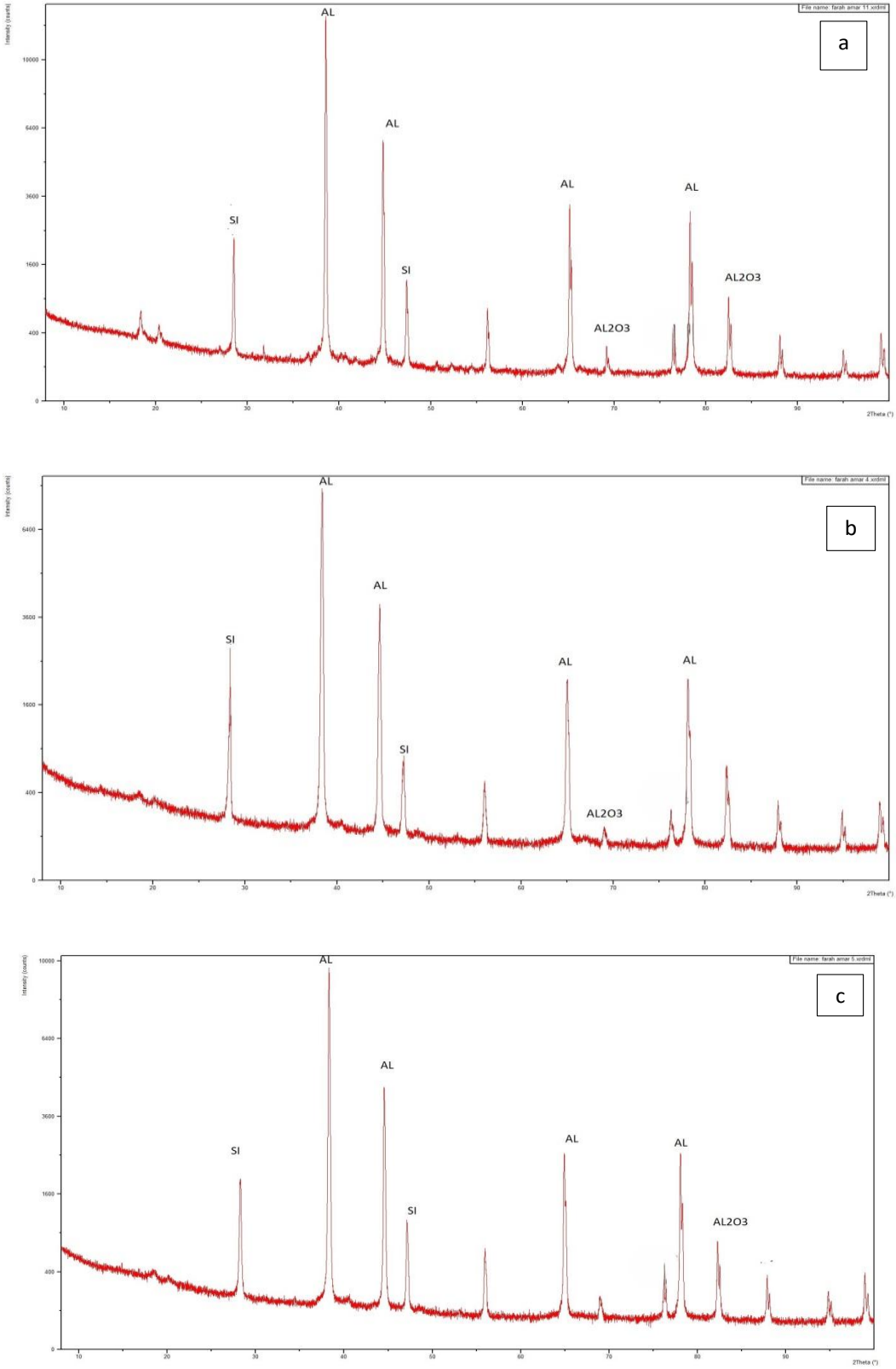

Fig 2. Show the Xrd analysis of Al-Si14% alloy with adding Al2O3;a- Al_2O_3 25 µm, b- Al_2O_3 50µm, Al_2O_3 100 µm Al_2O_3

Table 4 displays the intensities (I) and diffraction angle of the Al-Si alloy containing the additive Al_2O_3 at a particle size of 25 µm.

Alloy	phase	2 Theta	I/I1
Al-14%Si	Al	38.2, 44.5, 78.0	100, 50.77, 33.56
Al-14%Si	Si	28.2, 47.1	13.75, 11.46
Al-14%Si	AL2O3	.690, 82.2	33.56, 9.48

Table 5 displays the intensities (I) and diffraction angles of the Al-Si alloy containing the additive Al_2O_3 at a particle size of 50µm.

Alloy	phase	2 Theta	I/I1
Al-14%Si	Al	38.2, 44.6, 78.1	100, 46.93, 23.53
Al-14%Si	Si	28.3, 47.1, 76	13.75, 11.46
Al-14%Si	AL2O3	69.0,.822	1.58, 9.48

Table 6 displays the intensities (I) and diffraction angle of the Al-Si alloy containing the additive Al_2O_3 at a particle size of 100µm.

Alloy	phase	2 Theta	I/I1
Al-14%Si	Al	38.51, 44.76, 78.26	100, 47.76, 28.04
Al-14%Si	Si	28.48, 47.32,	14.09, 9.63,
Al-14%Si	AL2O3	69.17, 82.06,	1.51, 2.92

3.3 The Scanning Electron Microscope Result

The Scanning Electron Microscope provided further insights into the microstructure of the alloy, as demonstrated by the results shown in the test images. SEM images of the microstructures of the alloys before and after the addition of Al_2O_3 are shown in Figure 3.

According to the microstructural analysis, the particle size and processing parameters used during the stir casting process were directly related to the morphology, particle distribution, and grain refinement of the hypereutectic Al–14%Si alloy reinforced with varying alumina (Al_2O_3) particle sizes. Figures 1 and 3 offer important insights into the relationship between the reinforcement particle size and matrix uniformity by illustrating the microstructural evolution when the particle size is varied from 25 to 100 µm.

The typical hypereutectic microstructure of the unreinforced Al–14%Si alloy was characterised by coarse primary Si particles scattered throughout the Al matrix. Due to non-uniform stress transfer within the matrix, the coarse nature of silicon in hypereutectic alloys frequently results in heterogeneous mechanical behaviour [Nan Kang et al., 2016; S. K. Dey et al., 2009]. This morphology is consistent with the observations of Kang et al. (2016) and Dey et al. (2009).

Remarkable grain refinement was observed when $Al2O3_3$ particles were added, and the degree of refinement was higher for the alloys reinforced with 25 µm particles. The nucleation effect of fine $Al2O3_3$ particles, which served as heterogeneous nucleation sites during solidification, was responsible for this grain refinement. According to Saroj Kumar Sahu et al. (2022), who documented comparable enhancements in hypereutectic alloys reinforced with ceramic particles, this mechanism promotes the formation of a finer and more uniform microstructure [Sahu et al. 2022].

Despite some localised agglomeration, the distribution of $Al2O3_3$ within the matrix of the alloy reinforced with 50 µm particles remained relatively uniform and homogenous. According to Ashish Kumar et al. (2020), this behaviour is common when using intermediate particle sizes, where adequate particle wetting during stir casting is essential to achieve uniform dispersion. Although they did not attain the degree of homogeneity observed with the finer 25 µm particles, the presence of these somewhat dispersed particles partially refined the grains.

The alloy reinforced with 100 µm particles, on the other hand, showed more noticeable particle segregation and clustering. Clustering is caused by the poor wettability and greater inertia of larger particles during stirring, resulting in an uneven distribution across the matrix. According to Bharat Kumar and Menghani (2016), this type of segregation limits the gains in mechanical performance by decreasing the effective load transfer between the matrix and reinforcement [Bharat Kumar & Menghani, 2016]. Furthermore, as noted by Pitchayyapillai et al. (2017), localised particle clustering produces stress-concentration zones that may serve as sites for microcrack initiation under mechanical loading.

The fine Al2O3 particles were well integrated into the matrix, showing clean interfaces and little porosity, as further demonstrated by the scanning electron microscopy (SEM) images. This shows that the reinforcement and matrix are effectively bonded, which is necessary for better mechanical properties of the composites. Similar conclusions were reached by Bhutto et al. (2025), who found that finer particle sizes improved the interfacial strength by facilitating better wetting and distribution during the stir casting process [Bhutto et al., 2025].

Furthermore, it is well known that the microstructural refinement caused by the addition of Al2O33 contributes to the hindered dislocation motion during deformation. The elevated hardness values noted for the 25 μm-reinforced alloy are consistent with this mechanism, which is frequently referred to as the Orowan strengthening mechanism. According to Singhal et al. (2024) and Nordin et al. (2024), finer reinforcements improve the mechanical response by lowering the mean free path for dislocation glide and increasing the load transfer efficiency [Singhal et al., 2024; Nordin et al., 2024].

In conclusion, the microstructural analysis highlights that the highest hardness and wear resistance observed in the mechanical tests are supported by the most refined and uniform structure attained with 25 μm Al_2O_3 particles.

Although they were marginally less successful in producing a homogeneous microstructure, the 50 μm particles offered moderate refinement and an acceptable particle distribution. The poor distribution and clustering of 100 μm particles had a detrimental effect on the overall microstructural integrity and, consequently, the mechanical performance of the alloy. These results support earlier research by Nan Kang et al. (2016), Sahu et al. (2022), and Bhutto et al. (2025) that found particle size is a major determinant of the microstructural quality of hypereutectic Al–Si alloys. Fine particles improve interfacial bonding, nucleation, and grain refinement, resulting in superior mechanical properties in aluminum matrix composites.

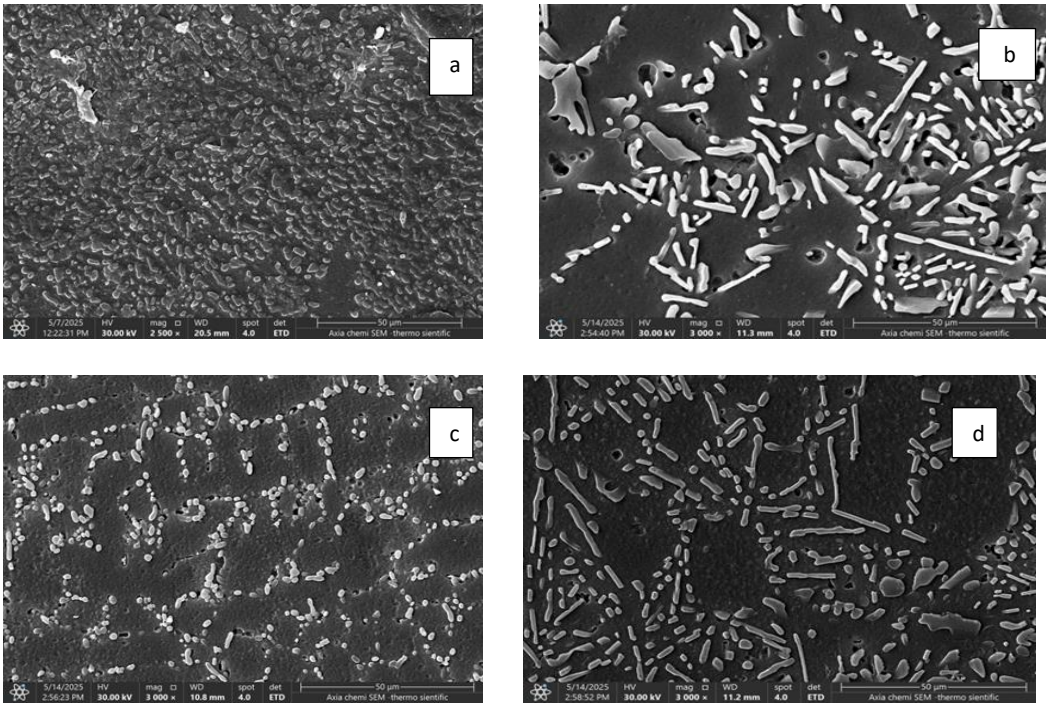

Figure (3) Scanning electron microscopy of alloys before and after addition of Al_2O_3,a) Al-14% alloy of Si, b) Al-14% alloy of Si with additive 25 μm Al_2O_3,c) Al-14% alloy of Si with additive50 μm Al_2O_3,d)Al-14% alloy of Si with additive100 μm Al_2O_3.

3.4 Result of hardness for AL-Si alloy

The size of the Al2O3 particles had a considerable impact on the hardness of the composites. Specifically, a reduction in the size of the reinforcement particles was correlated with an increase in hardness. As shown in Table 7, the composites reinforced with 25 μm Al_2O_3 exhibited the highest hardness values at 110 Hv, in contrast to those reinforced with 100 μm Al_2O_3 which showed the lowest hardness values at 95 Hv. Smaller reinforcement particles facilitate a greater contact area with the aluminum matrix, whereas larger particles result in a reduced contact area, which hinders diffusion. Additionally, the Al_2O_3 particles served as obstacles to dislocation movement within the Al matrix.

The hypereutectic Al–14%Si alloy reinforced with Al_2O_3 particles exhibited a hardness behaviour that illustrated the importance of the particle size and distribution within the aluminum matrix. The hypereutectic Al–Si matrix, characterised by coarse silicon particles scattered throughout the aluminum matrix, had a natural hardness of 92 HV, which was recorded by the base alloy without any Al_2O_3 addition. The hardness increased significantly with the addition of Al_2O_3 particles, reaching 110 HV for 25 µm particles, 105 HV for 50 µm particles, and a more modest improvement to 95 HV for 100 µm particles.

This increase in the hardness of alloys reinforced with finer particles can be attributed to several metallurgical mechanisms. First, the smaller 25 µm particles, which served as heterogeneous nucleation sites during solidification, exhibited a stronger grain refinement effect. In accordance with the Hall–Petch relationship, this leads to a finer and more homogeneous grain structure, which increases the hardness by lowering the mean free path of the dislocation motion. Second, the greater surface area of finer particles guarantees a stronger bond with the Al matrix. Enhanced interfacial adhesion offers two benefits: increased resistance to localised plastic deformation and improved load transfer during mechanical loading.

This process is also in line with Orowan strengthening, in which the tiny Al_2O_3particles obstruct the matrix's ability to dislocate the matrix. The hardness is improved as the material's resistance to deformation increases, and dislocations try to avoid these particles. A moderate hardness enhancement (105 HV) was observed for particles with a size of 50 µm. Despite the generally good dispersion, the overall effective surface area available for interfacial strengthening decreased owing to the localised agglomeration tendency.

The 100 µm particles, on the other hand, demonstrated the least amount of hardness improvement (95 HV). The effectiveness of the load transfer and strengthening mechanisms is limited by the larger particle size, which decreases the total interfacial area between the reinforcement and matrix. Furthermore, the SEM micrographs showed that these larger particles were distributed unevenly and clustered, resulting in weak spots in the matrix that adversely affected the hardness. Additionally, localised stress concentrations can be introduced by such clustering, which reduces the uniformity of the mechanical response to the load.

Prior research has extensively documented the robust relationship between microstructural homogeneity and hardness. For instance, finer Al_2O_3 particles result in a more homogeneous dispersion, enhanced interfacial bonding, and ultimately higher hardness values, as highlighted by Singhal et al. (2024) and Bhutto et al. (2025). Similarly, Nordin et al. (2024) observed that by reducing localised deformation and promoting a more uniform stress distribution under load, particle size reduction improved the effectiveness of the reinforcement in Al matrix composites. In conclusion, the particle size and dispersion quality attained during the stir casting process were directly related to the increase in hardness caused by the addition of Al_2O_3 particles. The 25 µm Al_2O_3 particles produced the most significant enhancement in hardness because of their superior ability to refine the grain structure and act as effective barriers to the dislocation motion. In contrast, the 100 µm particles provided minimal reinforcement owing to their poor dispersion and weak particle-matrix interfaces. This indicates that optimising the particle size is essential for optimising the mechanical performance of Al–Si–Al_2O_3 composites.

Table 7 Vickers hardness for alloy AL-14%SI (25,50,100) µm

Alloy	Befor addition Al_2O_3	With addition25 µm Al_2O_3	Withaddition50µm Al_2O_3	Withaddition100 µm Al_2O_3
Al-14%Si	**92**	**110**	**105**	**95**

3.5 Result of Wear

The research findings and calculated metrics were derived according to the experimental design. Subsequently, the results were evaluated using the commercial software MINITAB 20.4, which is specifically tailored for the experimental design and statistical analysis of experimental data. The experimental values pertaining to the wear rate Al_2O_3 with the calculated Signal to Noise Ratio (SNR) values for a specified response, as established by Equation 3, are displayed in Table 8.

According to the Taguchi design and statistical analysis (ANOVA), the wear behavior of the hypereutectic Al–14%Si alloy reinforced with Al_2O_3 particles showed a strong dependence on the reinforcement's particle size, as well as on the applied load and sliding time. Owing to its limited hardness (92 HV) and relatively coarse microstructure, the base alloy without reinforcement exhibited a higher wear rate. Wear resistance was considerably increased by the addition of Al_2O_3, with the 25 µm particles offering the greatest improvement, followed by the 50 and 100 µm particles, respectively.

Numerous strengthening mechanisms are responsible for the improvements in mechanical properties. Better load transfer during sliding conditions was ensured by a more even distribution of finer 25 µm particles within the aluminum matrix, which effectively increased the contact area. Strong barriers to material removal were created by tightly bound fine particles, which decreased abrasive wear and micro-cutting. The results of Sahu et al. (2022) and Bhutto et al. (2025), who found that a uniform dispersion of fine ceramic particles improves the wear resistance of Al–Si-based composites, are consistent with this behavior.

According to the statistical analysis using ANOVA, particle size was the most important factor affecting wear performance, followed by applied load, and time had the least effect in the experimental range. In the signal-to-noise (S/N) ratio analysis, the "smaller-is-better" principle indicated that decreasing the particle size consistently decreased the wear rate. This can be explained by the combined effects of the Orowan strengthening mechanism, enhanced interfacial bonding, and grain refinement, which increase the hardness and resistance to plastic deformation during sliding wear.

Owing to the increased frictional forces and matrix thermal softening at higher loads (15 N and 20 N), the wear rates increased for all samples; however, the alloys with 25 μm Al_2O_3 still exhibited superior resistance compared to those with larger particle sizes. However, due to particle clustering and non-uniform dispersion, which produced weak interfacial zones that served as starting points for surface damage and the spread of microcracks during sliding, the alloys reinforced with 100 μm particles exhibited lower wear resistance. Similar results from Pitchayyapillai et al. (2017) and Kumar and Menghani (2016), who found that larger particles resulted in inconsistent reinforcement effects and decreased tribological performance, support this observation.

The wear rate decreased as the hardness increased from 92 HV in the base alloy to 110 HV with the 25 μm particles, demonstrating a clear relationship between wear resistance and hardness. This indicates that surface hardness plays a direct role in preventing adhesive and abrasive wear. This relationship was further supported by a multiple linear regression model, which demonstrated that the wear performance was optimised by particle size reduction and moderate loading conditions.

In conclusion, by improving the hardness, stabilising the interfaces between the matrix and reinforcement, and refining the microstructure, the addition of Al_2O_3 increased the wear resistance of the Al–14%Si alloy. Owing to their superior dispersion and bonding, the alloys with 25 μm particles exhibited the lowest wear rates, whereas those with 100 μm particles exhibited a comparatively low wear resistance owing to clustering and a decrease in interfacial integrity. These findings are consistent with previous research, highlighting the importance of finely and evenly distributed ceramic particles in achieving high wear resistance in Al-Si- Al_2O_3 composites.

3.4.1 . Outcomes of the Statistical Evaluation of the Experiments

The research findings and calculated values were derived in accordance with the experimental design, followed by an analysis of the results using MINITAB 20.4, a commercial software specifically employed for experimental design and statistical analysis of the experimental apparatus. The impact of the regulated process parameters on the wear rate is visually illustrated in Figures 4 and 5, respectively. Through the examination of these findings, supported by the signal-to-noise ratio (SNR), the ideal conditions resulting in the wear rate are shown in Figures 4 and 5.

3.4.2 Wear Rate Variance Analysis

This analysis facilitated the identification of the comparative impact of the final parameter on the wear rate. Table 9 presents the variance analysis, including the P values and F-values, which illustrate the effectiveness of each individual parameter on the response characteristics, specifically the arithmetic value of the signal-to-noise ratio (SNR) and the mean wear rate. The P-value in Table 9 indicates the degree to which each parameter influences the associated response characteristics within the specified range. The findings indicate that parameter A is the most significant factor in achieving a minimal wear rate, whereas parameter B is the next most important factor for minimising the wear rate.

Wear rate variance analysis (ANOVA) provides an in-depth understanding of the ways in which particle size, applied load, and sliding time affect the wear performance of a hypereutectic Al–14%Si alloy reinforced with Al_2O_3. The statistical findings in Table 9 unequivocally show that the sliding time has the least impact on the wear rate, whereas the particle size has the largest impact, followed by the applied load.

This trend is supported by the p-values shown in the ANOVA table, which indicate that while time ($p = 0.004$) has a much smaller impact, it remains significant. Particle size ($p = 0.000$) and load ($p = 0.000$) had highly significant effects on the results of this study. Similarly, the F-values further demonstrate the importance of particle size, which had the highest F-value (16,957), followed by load (4,336), and time (244). These numbers unequivocally show that the most noticeable impact on increasing wear resistance is from decreasing the particle size. Microstructural observations support this, as Bhutto et al. (2025) and Sahu et al. (2022) reported that 25 μm particles produced a uniform and refined dispersion within the aluminum matrix, increasing the hardness and reducing surface degradation during sliding.

Samples reinforced with fine 25 μm Al_2O_3particles exhibited the lowest wear rates and highest tribological stability, according to the ANOVA results and the "smaller-is-better" criterion applied using the signal to noise (S/N) ratio. Because finer particles have a larger surface area, they improve interfacial bonding and facilitate more effective load transfer, which reduces microcutting and localised plastic deformation. Conversely, the wear resistance of the alloys reinforced with 50 and 100 μm particles improved less. In particular, under higher loads, the 100 μm particles exhibited poor particle clustering and distribution, resulting in weak spots in the microstructure that accelerated wear. This result confirms the findings of

Pitchayyapillai et al. (2017) and Kumar and Menghani (2016), who observed that larger reinforcement particles frequently led to lower wear resistance and an uneven stress distribution in aluminium-based composites.

Overall, the variance analysis emphasised the importance of particle size refinement in maximising the wear performance, followed by careful control of the load conditions. Although statistically significant, the sliding time had a secondary effect that mainly affected the surface temperature and caused slight matrix softening in situations involving prolonged wear. These findings demonstrate that the enhanced hardness, improved microstructural refinement, and stronger matrix–particle interfacial bonding all contribute to the superior performance of the 25 µm particles.

3.4.3 Multiple Linear Regression Models

A mathematical tool, MINITAB 20.4, was used to create the equation for multiple linear regression. A linear equation was used to fit the collected data to this model. This shows how the independent or predictor variable is linked to the answer obtained. The .following method was used to determine the wear rate

According to the multiple linear regression model created for this study, three important factors—the size of the Al_2O_3 particles, the applied load, and the sliding time— were directly correlated with the wear rate of the hypereutectic Al–14%Si alloy. The experimental data from the Taguchi L9 design were examined using MINITAB 20.4as show in the table(8,9,10,11) software, which demonstrated how these factors interacted to affect the wear performance of the composite.

The alloys reinforced with 25 µm Al_2O_3 particles consistently displayed the lowest wear rates, according to the results. The even dispersion throughout the matrix, robust particle-matrix bonding, and notable grain refinement are all responsible for this improvement, which increases the hardness and resistance to surface deterioration during sliding. Alloys with 100 µm particles exhibited higher wear rates owing to particle clustering and weaker interfacial bonding, which created localised weak points that were susceptible to surface damage under stress. In contrast, the samples reinforced with 50 µm particles exhibited moderate wear resistance owing to the less-uniform particle distribution.

It was also evident that the applied load had an effect on the results. Higher loads caused more material removal and surface damage, especially in samples with coarser particles, whereas lower loads reduced wear because of the lower frictional forces. Sliding time also had a secondary effect; longer exposures led to a slight increase in wear rates owing to matrix material softening and surface heating; however, this effect was less significant than that of particle size and load.

Overall, the regression analysis demonstrated that the sliding time had a relatively minor impact, and that the particle size was the most important factor, followed by the applied load. The model successfully predicted the wear behaviour under various circumstances, showing that uniformly distributed fine Al_2O_3 particles, moderate loads, and short sliding times resulted in the best wear performance. These results are consistent with previous research, including Singhal et al. (2024) and Bhutto et al. (2025), which emphasized the value of fine, evenly distributed reinforcements in enhancing the tribological characteristics of Al–Si-based composites.

wear rate=4.4367 - 0.1967 partical size_25 - 0.0133 partical size_50+ 0.2100 partical size_100 - 0.1200 load_10 + 0.0100 load_15 0.1100 load_20- 0.0333 time_10 - 0.0200 time_15 + 0.0533 time_20

Table 8. Orthogonal Array (L9) of Taguchi for Wear Test

Exp. No	Particle size (µm)	Load (N)	Time (min)	Wear rate * 10E-8 (g/cm)	Predicted of wear rate	SN
1	**25**	**10**	**10**	**3.12**	**3.11778**	**-9.8948**
2	**25**	**15**	**15**	**3.27**	**3.27111**	**-10.2849**
3	**25**	**20**	**20**	**3.43**	**3.43111**	**-10.7003**
4	**50**	**10**	**15**	**3.32**	**3.32111**	**-10.4172**
5	**50**	**15**	**20**	**3.47**	**3.46778**	**-10.8183**
6	**50**	**20**	**10**	**3.54**	**3.54111**	**-10.9740**
7	**100**	**10**	**20**	**3.67**	**3.67111**	**-11.2872**
8	**100**	**15**	**10**	**3.73**	**3.73111**	**-11.4286**
9	**100**	**20**	**15**	**3.90**	**3.89778**	**-11.8330**

Table 9 variance Analys

Source	DF	Adj SS	Adj MS	F	P
Partical size	**2**	**0.376822**	**0.188411**	**16957.00**	**0.000**
Load	**2**	**0.096356**	**0.048178**	**4336.00**	**0.000**

Source	DF	Adj SS	Adj MS	F	P
Time	2	0.005422	0.002711	244.00	0.004
Error	2	0.000022	0.000011		
Total	8	0.478622			

Table 10 Response Table for Mean

Level	Particle size	load	time
1	3.273	3.370	3.463
2	3.443	3.490	3.497
3	3.767	3.623	3.523
Delta	0.493	0.253	0.060
Rank	1	2	3

Table 11 Response Table for SN smaller is the best

Level	Particle size	load	time
1	-10.29	-10.53	-10.77
2	-10.74	-10.84	-10.85
3	-11.52	-11.17	-10.94
Delta	1.22	0.64	0.17
Rank	1	2	3

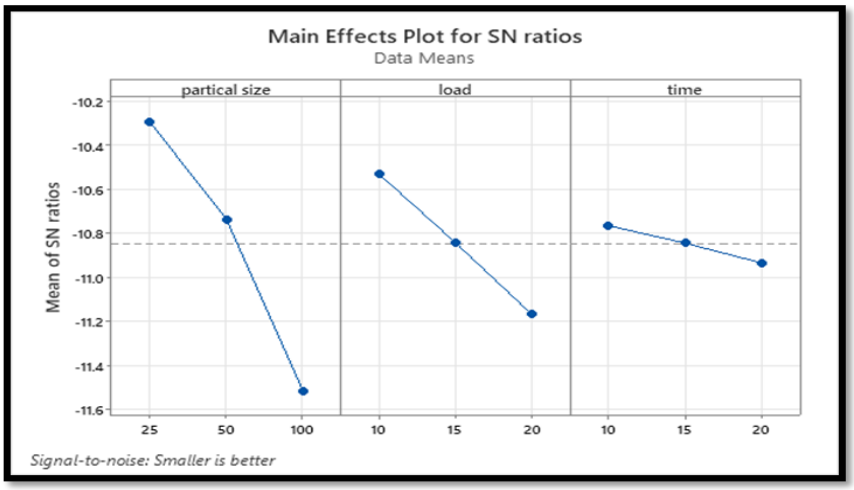

fig 4.Main Effected Plot for Main

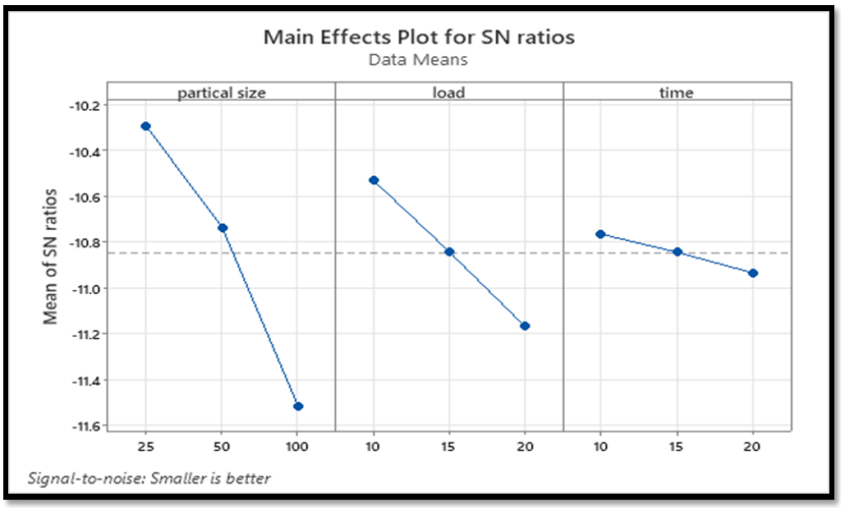

fig 5. Main Effected Plot for SN

3.4.4 Compare with previous studies

A direct numerical comparison with earlier studies on hypereutectic Al–Si alloys reinforced with Al_2O_3 or other ceramic particles was conducted to confirm the superiority of the current findings. The Vickers hardness of the composite reinforced with 25 µm Al_2O_3 particles reached 110 HV, as shown in Table 12. This is approximately 15–20% higher than the values reported by Bhutto et al. (2025) (~95 HV) under comparable processing conditions. Similarly, the wear rate in this study (3.12×10^{-8} g/cm for the best condition) showed superior tribological stability and was significantly lower than the values reported by Sahu et al. (2022) and Singhal et al. (2024). These results demonstrate that increasing the hardness and wear resistance requires careful consideration of particle size optimization.

Table 12 Comparative Results of Previous Studies.

Study	Reinforcement Type	Hardness (HV)	Wear Rate ($\times 10^{-8}$ g/cm)
Present study (25 µm)	**Al_2O_3 (3 wt.%)**	**110**	**3.12**
Bhutto et al. (2025)	**Al_2O_3 (3 wt.%)**	**95**	**3.90**
Sahu et al. (2022)	**Al_2O_3 (3 wt.%)**	**102**	**3.67**
Singhal et al. (2024)	**Natural minerals**	**100**	**3.54**

4. Applications

Hypereutectic Al–14%Si alloys reinforced with Al_2O_3 particles can be used in a wide range of industrial and engineering applications when high wear resistance, dimensional stability, and thermal conductivity are required.

Because of its increased hardness and resistance to wear, the composite is an excellent option for important parts such as rocker arms, brake rotors, cylinder liners, pistons, and valve guides in the automotive industry. In high-temperature and high-load settings, the fine dispersion of Al_2O_3 particles ensured a longer service life by strengthening the matrix and reducing the wear rate of the composite. This is consistent with earlier research showing that, compared with traditional aluminum alloys, hypereutectic Al–Si alloys with ceramic reinforcement perform better in internal combustion engines.

The alloy is used in the aerospace industry for parts such as bearing housings, gear components, and structural fittings that require both low density and superior wear properties owing to its high strength-to-weight ratio and resistance to thermal fatigue. In these high-precision applications, where dimensional stability under cyclic thermal and mechanical loads is crucial, a refined microstructure produced with finer particle reinforcement (25 µm) is particularly advantageous.

This composite has potential applications in the manufacturing and tooling sectors, particularly in wear-resistant tooling components, die inserts, and extrusion dies. The uniform dispersion of Al_2O_3 resulted in improved surface hardness and decreased friction loss, which reduced maintenance costs by extending the operational lifespan and minimising tool wear.

Additionally, the enhanced stability and wear performance of this material make it a promising choice for marine applications, including parts for watercraft engines, pumps, and valves that are subjected to corrosive and abrasive conditions. Durability and dependability under demanding service conditions are guaranteed by improved mechanical strength and corrosion resistance of the coating.

According to sustainability theory, the ability to maximise the mechanical performance of Al–Si alloys through economical stir casting provides a competitive edge in creating lightweight and robust materials without the need for costly manufacturing processes. This creates the possibility of increasing production to satisfy the rising demand for lightweight and high-performance components in contemporary energy and transportation systems. These composites may also be modified for hybrid casting-processing or additive manufacturing techniques in the future, allowing the creation of intricate geometries with customised microstructures for extremely specialised applications.

5. Conclusion

The study showed that the mechanical and tribological properties of a hypereutectic Al–14%Si alloy were significantly improved by reinforcing it with Al_2O_3 particles using the stir casting technique. Microstructural analysis revealed that the 25 µm Al_2O_3 particles achieved the most uniform distribution and effective bonding within the aluminum matrix, resulting in significant grain refinement and a more homogenous structure. The highest hardness value of 110 HV and the lowest wear rate were directly attributed to this refinement, demonstrating a close correlation between wear resistance and surface hardness. According to the Taguchi design and

ANOVA, the particle size was the most important factor in minimising wear, followed by the applied load, and sliding time had the least significant but still discernible impact. The resistance of the material to plastic deformation and micro-cutting during sliding was improved by the improved interfacial bonding and load transfer of fine particles. Conversely, the use of larger particles (100 μm) resulted in weaker interfaces, poor dispersion, and clustering, which decreased the hardness and increased the wear rates.

Overall, the findings confirm that optimising the particle size is crucial for achieving superior mechanical performance in Al–Si–Al_2O_3 composites. These composites are ideal for demanding engineering applications that require high durability and stability, as they combine fine particles, moderate loads, and controlled processing parameters to provide the best balance of hardness, wear resistance, and structural integrity of the composite.

6. Future works

Although this study effectively showed that hypereutectic Al–14%Si alloys reinforced with Al_2O_3 particles exhibited significantly improved hardness and wear resistance, several areas still need to be investigated to increase the knowledge of the industrial applicability of these composites.

To determine the ideal content that strikes a balance between mechanical strength, ductility, and cost-effectiveness, future research should focus on different reinforcement ratios outside the 3 wt percent used in this study. Investigating nanosized Al_2O_3 particles may also shed light on the advantages of a larger bonding surface area, which could result in improved wear resistance and further grain refinement of the coating.

To gain a deeper understanding of the interfacial bonding between the Al_2O_3 particles and Al–Si matrix, as well as the function of dislocation interactions in strengthening mechanisms, advanced characterisation techniques such as transmission electron microscopy (TEM), electron backscatter diffraction (EBSD), and microhardness mapping can be used.

More useful information for industrial applications in the automotive, aerospace, and marine sectors can be obtained by examining the performance of these composites under various loading and environmental conditions, such as high temperatures, lubricated wear, and corrosive environments. In a similar vein, future research should incorporate fatigue and impact tests to assess the structural integrity and long-term dependability under dynamic loading.

Future research could examine ways to improve particle dispersion and reduce porosity by modifying the stir casting technique, such as by adjusting the stirring time, speed, and thermal profile, or by combining stir casting with electromagnetic or ultrasonic stirring.

Finally, experimental work can be combined with computational modelling and finite element simulations to predict the wear mechanisms, stress distribution, and microstructural evolution under various circumstances. The design of optimized Al–Si–Al_2O_3 composites for high-performance applications can be accelerated using this approach.

Acknowledgments

The facilities, technical assistance, and laboratory supplies required to conduct this study were provided by Mustansiriyah University in Baghdad, Iraq, for which the authors are grateful to the university. Their unwavering support and encouragement were crucial for the successful completion of this research.

References

- Abuzinadah, A. J., Merdad, Y. M. A., Aldharrab, R. S., Almutairi, W. A., Yeslam, H. E., & Hasanain, F. A. (2024). Microhardness and compressive strength of bulk fill glass hybrid material and other direct restorative materials. *Journal of Composites Science, 8*(12), 508. https://doi.org/10.3390/jcs8120508
- Bhutto, A. A., Wahab, S. B., Solangi, F. A., Hussain, F., Zhou, D., Khan, T. M. Y., & Shaik, A. S. (2025). Microstructure, mechanical and physical characteristics analysis of ADC14 hypereutectic AlSi composite reinforced with Al_2O_3. *Alexandria Engineering Journal, 126*(7), 303–319. https://doi.org/10.1016/j.aej.2025.04.072
- Chandra Sekhar Rao, P. V., Satya Devi, A., & Basava Kumar, K. G. (2012). Influence of melt treatments on dry sliding wear behavior of hypereutectic Al-15Si-4Cu cast alloys. *Jordan Journal of Mechanical & Industrial Engineering, 6*(1), 55–61.
- Das, D. K., Mishra, P. C., Singh, S., & Pattanaik, S. (2014). Fabrication and heat treatment of ceramic-reinforced aluminium matrix composites – A review. *International Journal of Mechanical and Materials Engineering, 9*(1), 6. https://doi.org/10.1186/s40712-014-0006-7

- Dey, S. K., Perry, T. A., & Alpas, A. T. (2009). Micromechanisms of low load wear in an Al–18.5% Si alloy. *Wear, 267*(1), 515–524. https://doi.org/10.1016/j.wear.2008.11.011
- Elil Raja, D., Vijayan, S., Sonar, T., & Prathap Singh, S. (2024). Analyzing the dry sliding wear performance on aluminum 6061 alloy reinforced with SiC and B4C hybrid nanocomposite. *Advances in Materials Science, 24*(4), 42–56. https://doi.org/10.2478/adms-2024-0022
- Gope, R., Saini, D. K., Ganguly, S., & Mandal, A. (2024). Investigating the load and temperature-dependent dry sliding wear performance of Al–12Ce alloys with Si and Mg additions. *Wear, 544–545*, 205315. https://doi.org/10.1016/j.wear.2024.205315
- Kang, N., Coddet, P., Liao, H., Baur, T., & Coddet, C. (2016). Wear behavior and microstructure of hypereutectic Al–Si alloys prepared by selective laser melting. *Applied Surface Science, 378*(8), 142–149. https://doi.org/10.1016/j.apsusc.2016.03.221
- Khan, A. H., Shah, S. A. A., Umar, F., Noor, U., Gul, R. M., Giasin, K., & Aamir, M. (2022). Investigating the microstructural and mechanical properties of novel ternary reinforced AA7075 hybrid metal matrix composite. *Materials, 15*(15), 5303. https://doi.org/10.3390/ma15155303
- Kumar, A., Singh, R. C., & Chaudhary, R. (2020). Recent progress in production of metal matrix composites by stir casting process: An overview. *Materials Today: Proceedings, 21*(3), 1453–1457. https://doi.org/10.1016/j.matpr.2019.10.079
- Kumar, B., & Menghani, J. V. (2016). Aluminium-based metal matrix composites by stir casting: A literature review. *International Journal of Materials Engineering Innovation, 7*(1), 1–14. https://doi.org/10.1504/IJMATEI.2016.077310
- Lasa, L., & Rodriguez-Ibabe, J. M. (2003). Wear behaviour of eutectic and hypereutectic Al–Si–Cu–Mg casting alloys tested against a composite brake pad. *Materials Science and Engineering: A, 363*(1), 193–202. https://doi.org/10.1016/S0921-5093(03)00633-6
- Muhammad Faiz Abdul Razak, M., Osman, S. A., Ourdjini, A., & Osman, S. A. (2024). Comparative analysis of aluminium 6061-T6 with different stock leaves setting on holes true position: A case study. *Journal of Advanced Research in Applied Mechanics, 128*(1), 138–151. https://doi.org/10.37934/aram.128.1.138151
- Muhammad Haziq, I., Shafie, K., Hafis, S. M., Nor Aiman, S., Ahmad, A. Z. A., & Hizam Md, Y. A. S. (2023). Effects of coating and lubrication on friction and wear for metal-to-metal application. *Journal of Advanced Research in Applied Mechanics, 110*(1), 52–62. https://doi.org/10.37934/aram.110.1.5262
- Muhammad Hisyamuddin Rosli, M., Zailani, Z. A., Shuaib, N. A., Zainuddin, M. Z., & Azawqari, A. A. (2025). Optimisation of cutting performance in drilling of aluminium alloy 7075 involving chilled air cooling under Taguchi method. *Journal of Advanced Research in Applied Mechanics, 133*(1), 12–23. https://doi.org/10.37934/aram.133.1.1223
- Nordin, A. F., Nasir, N. F., Osman, S. A., Ramesh, S., & Adbulkareem, A. N. (2024). Review of aluminium (AA6061) metal matrix composite (MMC) by stir casting method. *Journal of Advanced Research in Applied Mechanics, 128*(1), 115–128. https://doi.org/10.37934/aram.128.1.115128
- Pitchayyapillai, G., Seenikannan, P., Balasundar, P., & Narayanasamy, P. (2017). Effect of nano-silver on microstructure, mechanical and tribological properties of cast 6061 aluminum alloy. *Transactions of Nonferrous Metals Society of China, 27*(10), 2137–2145. https://doi.org/10.1016/S1003-6326(17)60239-5
- Qian, Z., Liu, X., Zhao, D., & Zhang, G. (2008). Effects of trace Mn addition on the elevated temperature tensile strength and microstructure of a low-iron Al–Si piston alloy. *Materials Letters, 62*(14), 2146–2149. https://doi.org/10.1016/j.matlet.2007.11.035
- Radhika, N., Jojith, R., Vignesh, S., Raghavenderen, H. S., Abinav, S., & Adediran, A. A. (2024). Characterization, mechanical properties, and wear behavior of functionally graded aluminum hybrid composite. *Scientific Reports, 14*(1), 19509. https://doi.org/10.1038/s41598-024-70189-w
- Rumi, M. J. U., & Rahman, M. M. (2023). Characterization on specific wear rate of Al composite reinforced with nano-Al_2O_3 using Taguchi's technique. *Tribologia – Finnish Journal of Tribology, 40*(1–2), 37–45. https://doi.org/10.30678/fjt.125959
- Sahu, S. K., Patra, R. K., & Majhi, J. (2022). Effect of addition of 3% Al_2O_3 on mechanical and microstructural properties in Al-16Si hypereutectic alloys with pouring temperature. *Materials Today: Proceedings, 62*(10), 5850–5855. https://doi.org/10.1016/j.matpr.2022.03.517
- Singhal, V., Shelly, D., Babbar, A., Lee, S.-Y., & Park, S.-J. (2024). Review of wear and mechanical characteristics of Al–Si alloy matrix composites reinforced with natural minerals. *Lubricants, 12*(10), 350. https://doi.org/10.3390/lubricants12100350
- Subramanian, S., Sendrayan, V., Pachaiyappan, K., & Balashanmuganath, S. B. (2025). Optimization of wear behaviour of Al6061 metal matrix composites using Taguchi approach. *Turkish Journal of Engineering, 9*(1), 56–63. https://dergipark.org.tr/en/pub/tuje
- Tirfe, D., Woldeyohannes, A. D., Hunde, B. R., Batu, T., & Geleta, E. (2024). Optimizing the dry sliding wear behavior of stir-casted Al6061/nano-Al_2O_3/quartz hybrid metal matrix composite using Taguchi method. *Advances in Tribology, 2024*, Article ID 3589701, 14 pages. https://doi.org/10.1155/2024/3589701
- Wang, Q. Z., Lin, X., Wen, X. L., Kang, N., & Huang, W. D. (2020). Microstructure and wear behavior of nano-TiB_2p/2024Al matrix composites fabricated by laser direct energy deposition with powder feeding. *Journal of Tribology, 143*(5), 051101. https://doi.org/10.1115/1.4048551